*Int. J. Heat Mass Transfer.* Vol. 14, pp. 207–221. Pergamon Press 1971. Printed in Great Britain

# THE STABILITY OF A FLUID LAYER SUBJECTEDTO A STEP CHANGE IN TEMPERATURE: TRANSIENT VS. FROZEN TIME ANALYSES.

P. M. GRESHO* and R. L. SANI

Department of Chemical Engineering, University of Illinois, Urbana, Illinois, U.S.A.

(*Received* 25 *March* 1970 *and in revised form* 5 *May* 1970)

**Abstract**—The linearized behavior of a fluid layer subjected to a step change in surface temperature is examined using two different conceptual approaches. The first approach uses initial value techniques while the second employs two common versions of the "frozen-time" hypothesis. Both surfaces are taken as rigid and conducting. Galerkin's method is used to obtain the approximate solutions, while "exact" solutions are obtained via numerical integration for certain cases.

It is shown that, while the first version of the frozen time model (the marginal state analysis) is not applicable to the transient system, the second version (quasi-static analysis) is valid for large time but is of limited usefulness for most cases of interest. The effects of various initial conditions, on the velocity and temperature perturbations, are clarified and discussed. The results presented here complement those available for a semi-infinite fluid with the same boundary conditions at he top surface.

## NOMENCLATURE

**A**, matrix with elements $A_{ij}$ defined in Section 3;
$\boldsymbol{a}$, dimensionless wave vector;
$a$, magnitude of $\boldsymbol{a}$;
$a_x, a_y$, components of $\boldsymbol{a}$;
**B**, matrix with elements $B_{ij}$ defined in Section 3;
**C**, matrix with elements $C_{ij}$ defined in Section 3;
**D**, matrix with elements $D_{ij}$ defined in Section 3;
**E**, matrix with elements $E_{ij}$ defined in Section 3;
erf, error function;
$f_i$, $z$-part of temperature trial functions $\equiv \sin i\pi z$;
$g$, acceleration due to gravity;
$h$, layer depth;
$Pr$, Prandtl number $\equiv \nu/\kappa$;
$Q$, dimensionless heat source defined in Section 2;
$R$, Rayleigh number $\equiv \alpha g \Delta T h^3/\kappa\nu$;
$t'$, time;
$t$, dimensionless time $\equiv t'\kappa/h^2$;
$T'$, temperature $\equiv \Delta T[T + \theta/\sqrt{R}]$;
$\bar{T}'$, base (no flow) temperature;
$\bar{T}$, dimensionless temperature $\equiv \bar{T}'/\Delta T$;
$T_i$, time dependent amplitude in equation (15);
$V_i$, time dependent amplitude in equation (16);
$w'$, vertical component of velocity;
$w$, dimensionless vertical component of velocity $\equiv w'h/\kappa$;
$x', y', z'$, position coordinates;
$x, y, z$, dimensionless position coordinates $\equiv x'/h, y'/h, z'/h$.

Greek symbols

$\alpha$, thermal coefficient of expansion;
$\theta'$, temperature perturbation;
$\theta$, dimensionless temperature perturbation $\equiv \theta(\sqrt{R})/\Delta T$;
$\kappa$, thermal diffusivity;
$\nu$, kinematic viscosity;

* Presently with the Atomics International Division of North American Rockwell Corporation.

$\sigma$, growth factor appearing in equations (11) and (12);
$\phi_i$, $z$-part of vertical velocity trial functions $\equiv \sin \pi z \sin i\pi z$.

Special symbols
$\mathscr{F}(f)$, two dimensional Fourier transform of $f$;
overdot, time differentiation;
overbar, root mean square average;
$\Delta T$, temperature difference across layer.

## 1. INTRODUCTION

THE STABILITY of a quiescent, horizontal, fluid layer, cooled uniformly from above, whose density decreases linearly with increasing temperature can be adequately assessed by the magnitude of a dimensionless group, $R$, called after Rayleigh. If the Rayleigh number exceeds the critical value (1707·76 in this investigation), the "top-heavy" quiescent fluid layer becomes unstable, flow begins (usually tending to some steady, cellular convection pattern in the horizontal plane), and the temperature profile becomes distorted due to convection. If, in an experiment, the Rayleigh number is increased very slowly (e.g. by lowering the temperature at the top surface while maintaining the bottom temperature), it is found that the linearized theory corresponding to a constant temperature gradient does indeed describe, to a good approxition, the stability of the layer and the size of the resulting convection cells. A thorough summary of this hydrodynamic stability is given in Chandrasekhar [1]. However, if an experiment is performed wherein the Rayleigh number is quickly increased from zero (a layer of uniform temperature) to a value above critical, the time at which (measurable) motion begins—the onset time—becomes the dominant question. This stability problem, i.e. with a time-dependent, non-linear base temperature profile, has only recently been attacked analytically and is not yet nearly as well resolved as the steady (linear profile) case. The early investigators [2–4, 6] of this transient problem took the approach of modifying the extant hydrodynamic stability analyses (i.e. for non-transient systems) in such a way (viz, by "freezing" the time) as to retain the basic concepts and methods underlying these analyses. The first examination to start afresh and properly consider the problem as an initial value problem was performed by Foster [5] while another (Robinson [7]) examines the range of validity of the frozen time model, based in part on Foster's work. Some recent papers using initial value techniques are those by Foster [8], Mahler *et al.* [9] and Elder [10].

The purpose of this investigation is to clarify and to critically examine the models employing the frozen time assumption. The system considered in this study is one with fixed temperatures (uniform throughout for time less than zero) at top and bottom surfaces (conducting walls); these surfaces are rigid and are assumed to be "no-slip" with respect to fluid motion. The layer has a finite depth and is infinite in the horizontal directions. At time zero, the upper surface temperature is reduced to $\Delta T$ below the lower one and maintained there.

## 2. BASIC EQUATIONS

The derivation of the governing equations has been adequately presented several times (cf. Goldstein, Chandrasekhar, Foster) and will not be repeated here. For a mechanically incompressible but thermally deformable fluid these (linearized and dimensionless) equations are as follows ($z$ is measured vertically down):

$$\frac{\partial \bar{T}}{\partial t} = \frac{\partial^2 \bar{T}}{\partial z^2} \tag{1}$$

$$\left(\frac{\partial}{\partial t} - \nabla^2\right)\theta = -(\sqrt{R})w\frac{\partial \bar{T}}{\partial z} \tag{2}$$

$$\left(\frac{1}{Pr}\frac{\partial}{\partial t} - \nabla^2\right)\nabla^2 w = -(\sqrt{R})\nabla_2^2\,\theta.$$

The initial condition and boundary conditions on the base temperature are:

$$\bar{T} = 1; \qquad 0 \leqslant z \leqslant 1; \qquad t = 0 \tag{4}$$

$$\left.\begin{aligned} \bar{T} &= 0; \quad z = 0; \quad t > 0 \\ \bar{T} &= 1; \quad z = 1; \quad t \geqslant 0 \end{aligned}\right\}. \tag{5}$$

For a system with conducting walls at both surfaces the boundary conditions on the temperature perturbation are $\theta = 0$ at $z = 0, 1$ while those on the velocity perturbation are, for rigid walls $w = 0$ and $\partial w/\partial z = 0$ at $z = 0, 1$. The initial conditions for the perturbations will be discussed later.

The solution to (1) subject to (4) and (5) is:

$$\bar{T} = z + \frac{2}{\pi}\sum_{n=1}^{\infty}\frac{\sin n\pi z}{n}.\exp\left[-n^2\pi^2 t\right]. \tag{6}$$

at small times ($t < \sim 0{\cdot}01$) the following approximation, based on the fluid having infinite depth, is more useful:

$$\bar{T} = \operatorname{erf}(z/\sqrt{4t}). \tag{7}$$

Since there are no lateral boundaries on the system, an arbitrary distrubance in the $xy$-plane can be expressed in terms of two-dimensional periodic waves by means of Fourier transformations; e.g.

$$\mathscr{F}[f(x, y, z, t)] \equiv f_1(a_x, a_y, z, t)$$

$$= \frac{1}{2\pi}\int_{-\infty}\int_{-\infty} f(x,y,z,t).\exp\left[i(a_x x + a_y y)\right]\mathrm{d}x\mathrm{d}y, \tag{8}$$

where $a \equiv \sqrt{(a_x^2 + a_y^2)}$ is the dimensionless horizontal wave number of the disturbance. Transforming (2) and (3) according to (8) and noting that

$$\left.\begin{aligned} \mathscr{F}[\nabla_2^2 w] &= -a^2 w_1 \\ \mathscr{F}[\nabla_2^2 \theta] &= -a^2 \theta_1 \end{aligned}\right\} \tag{9}$$

leads to the following equations,

$$\frac{\partial\theta_1}{\partial t} = \left(\frac{\partial^2}{\partial z^2} - a^2\right)\theta_1 - (\sqrt{R})\, w_1 \frac{\partial\bar{T}}{\partial z} \tag{10}$$

$$\frac{1}{Pr}\left(\frac{\partial^2}{\partial z^2} - a^2\right)\frac{\partial w_1}{\partial t} = \left(\frac{\partial^2}{\partial z^2} - a^2\right)^2 w_1 + a^2(\sqrt{R})\,\theta_1. \tag{11}$$

While the boundary conditions are unaffected, the initial conditions must in general be considered in terms of the transform variables, $a_x$ and $a_y$.

Since $\partial\bar{T}/\partial z$ is a function of $t$, the time-dependence cannot be separated by assuming $\partial/\partial t = \sigma$, where $\sigma$ is the growth rate. However, for the linear temperature profile, $\partial\bar{T}/\partial z = 1$ and exponential time dependence is correct, giving (henceforth the subscripts will be suppressed):

$$\sigma\theta = (D^2 - a^2)\,\theta - (\sqrt{R})\, w \tag{12}$$

$$\frac{\sigma}{Pr}(D^2 - a^2)w = (D^2 - a^2)^2 w + a^2(\sqrt{R})\theta. \tag{13}$$

This is in the form of the classical stability equations, leading to an eigenvalue problem for $R$ (or $\sigma$).

At this point, the two variants of the "frozen time" model can be introduced; the first is the marginal state model and the second is the quasi-static or asymptotic model.

In the marginal state method the nonlinear base temperature profile is "frozen" at each instant of time. In this case $\partial\bar{T}/\partial z$ is only a function of $z$ and $t$ is a parameter and the variables can be separated as in the case of the linear profile. The problem is then reduced to a classical hydrodynamic stability problem, albeit one with a nonlinear temperature profile. On the other hand, the asymptotic model is based on the hypothesis that after some time, sufficiently large, the growth rate of the perturbations is so large relative to the rate of change of the base profile (which approaches zero at infinite time) that the perturbations can be treated as being "in equilibrium" with the existing base profile at each instant. Unfortunately, the requirement of "large time" will be shown to severely restrict the applicability of this model.

### 3. FORMULATION OF THE APPROXIMATE SOLUTION EQUATIONS

Equations (10) and (11) must be integrated, subject to initial conditions on $\theta$ and $w$, for

various values of $R$, $Pr$ and $a^2$, in order to obtain a transient "stability map" of the system. This will be done approximately using a time-dependent Galerkin method; the temperature and velocity perturbations are thus each represented by a series of specified spatial functions (trial functions) with time-dependent amplitude coefficients. The determination of these amplitude coefficients constitutes the bulk of the solution method since the spatial dependence is "removed" according to the method of Galerkin, Thus,

$$\theta(z, t) = \sum_{i=1}^{N} T_i(t)\, f_i(z), \tag{14}$$

$$w(z, t) = \sum_{i=1}^{N} V_i(t)\, \varphi_i(z) \tag{15}$$

where, for this study, $f_i(z) = \sin i\pi z$ and $\varphi_i(z) = \sin \pi z \sin i\pi z$, which satisfy the boundary conditions on $z$. Galerkin's method results in a linear set of $2N$ simultaneous, first-order differential equations for the amplitude coefficients, $V_i(t)$ and $T_i(t)$, the Galerkin equations of the problem ($\dot{T}_i \equiv (\mathrm{d}T_i/\mathrm{d}t)$, etc.):

$$\dot{\boldsymbol{T}} = -[\mathbf{A}.\boldsymbol{T} + (\sqrt{R})\,\mathbf{B}(t).\boldsymbol{V}] \tag{16}$$

$$\frac{1}{Pr}\,\mathbf{C}.\dot{\boldsymbol{V}} = -[\mathbf{D}.\boldsymbol{V} + a^2(\sqrt{R})\,\mathbf{E}.\boldsymbol{T}]. \tag{17}$$

Once initial conditions are specified for $T_i$, $V_i$, $i = 1,2,\ldots,N$, the set of equations (16), (17) may be integrated simultaneously. This was done numerically on an IBM 7094 using a 4th-order Runge–Kutta method.

The characteristic equation generated in the asymptotic (large time) model can be obtained by formally setting $\dot{\boldsymbol{T}} = \sigma\boldsymbol{T}$ and $\dot{\boldsymbol{V}} = \sigma\boldsymbol{V}$ in (16) and (17) and satisfying the solvability condition for the resulting set of algebraic equations, i.e.

$$\det\left|\frac{\sigma}{Pr}\mathbf{C} + \mathbf{D} - a^2 R\,\mathbf{E}.(\mathbf{A}+\sigma\mathbf{I})^{-1}.\mathbf{B}(t)\right| = 0. \tag{18}$$

The characteristic equation generated by the marginal state model is obtained by simply setting $\sigma = 0$ in (18).

## 4. NUMERICAL SOLUTION OF THE APPROXIMATE EQUATIONS

Since the linearized equations describing the perturbations, (2) and (3), and the boundary conditions, are homogeneous, a solution can be obtained only up to an arbitrary multiplicative constant. The selection of this "constant" adds another complication to the analysis. One obvious and simple way of avoiding (or disguising) this selection is to somehow normalize the results based on the initial conditions. Although this procedure is quite acceptable mathematically, it does little to aid one's physical concept of the system. Since no better way is known, the results will be presented in a normalized form. Among the reasonable quantities to be considered for normalization are the following: (1) average velocity, average temperature, or a combination of the two, (2) RMS (root mean square) velocity, RMS temperature, or a combination of the two (e.g. the vitality—a measure of the "energy" of the perturbations defined as

$$V(t) \equiv \frac{1}{2}\int_{\mathrm{Vol}} \left\{\frac{1}{Pr}[u^2 + v^2 + w^2] + \theta^2\right\} \mathrm{d}v.$$

However, in order to allow a more direct comparison of our results with those of Foster and of Mahler *et al.*, we will measure the instability of the system in terms of a normalized, RMS velocity (or kinetic energy), $\bar{w}(t)$:

$$\bar{w}(t) = \left[\frac{\int_0^1 w^2(z, t)\,\mathrm{d}z}{\int_0^1 w^2(z, 0)\,\mathrm{d}z}\right]^{\frac{1}{2}}. \tag{19}$$

Note that the initial velocity perturbation must be non-zero, a restriction not encountered if the vitality were selected instead.

The onset time is then "defined" from the value of $\bar{w}(t)$ at which infinitesimal disturbances

become observable and is thus directly related to the elusive ratio introduced above. Based partly on intuition and partly on precedent, a value of 1000 was used in this work; i.e. the onset time is defined by $\bar{w}(t_c) = 1000$.

The general nature of the solutions, $\theta$ and $w$, and their shape and growth relative to $\bar{T}(z, t)$ are displayed in Figs. 1 and 2 for symmetric initial

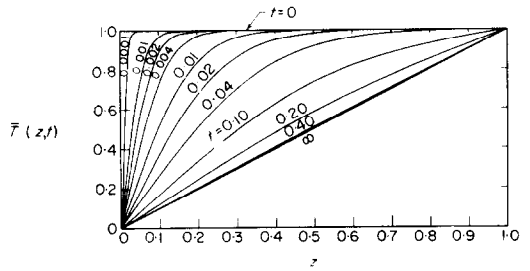


FIG. 1. The base temperature profile for a step change.

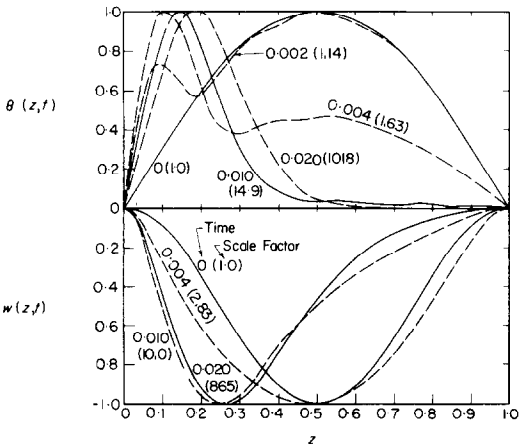


FIG. 2. $Z$-profiles at various times for $R = 10^5$, $Pr = 7$, $a = 7{\cdot}8$, $N = 10$. The RMS velocity, $\bar{w}(t)$, at times 0, 0·002, 0·004, 0·010, 0·020 is 1·0, 2·75, 3·18, 14·9 and 753 respectively.

profiles ($V_1 = 1$, $T_1 = -1$). The temperature profile near the onset time (i.e. at $t = 0{\cdot}02$) is seen to be independent of the lower boundary, whereas the velocity profile is still slightly affected; hence, $R = 10^5$ and $Pr = 7$ should be close to "borderline" between treating the layer as one of finite or infinite depth. It is also noteworthy that a reasonable accuracy was obtained if the number of trial functions in each expansion was at least as large as the wave number, $a$. This result was also observed by Foster and Mahler *et al.*

The initial value problem can only be solved after specifying "initial" data; these data determine on which trajectory the solution lies. In the case of a fluid layer heated from below, the initial conditions are generally not known and to some extent are even beyond the control of the

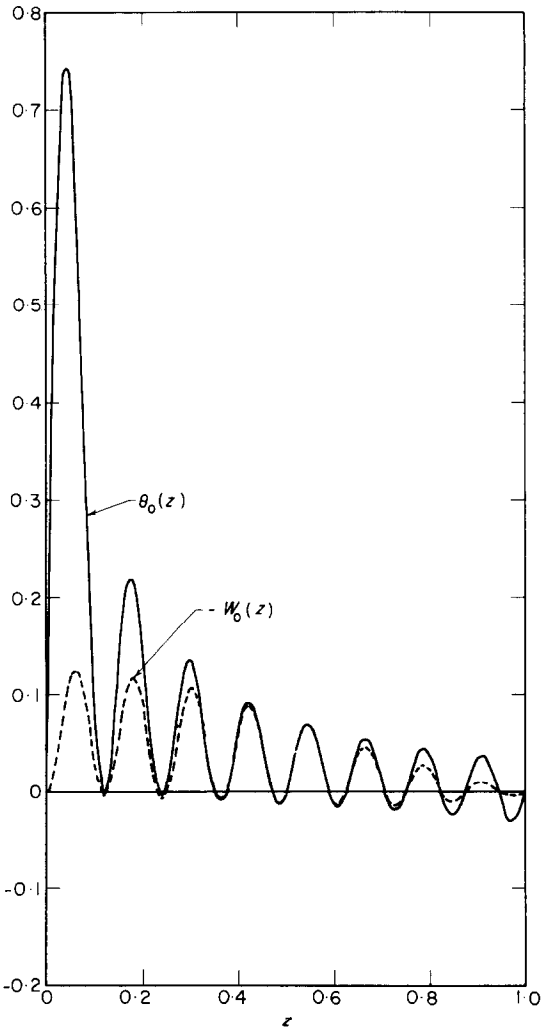


FIG. 3. White noise initial conditions ($N = 16$); the curves are given by

$$\theta_0(z) = \frac{1}{N}\sum_{n=1}^{\frac{1}{2}} \sin n\pi z \quad \text{and} \quad w_0(z) = -\theta_0 \sin \pi z.$$

experimenter. (Here, initial conditions refer to the distribution of perturbation temperature and velocity, generally at the time the step change is imposed.) In fact, it is not even known whether initial conditions are the most important reason for instability in the laboratory—equally possible are continuous (in time), random (or not) perturbations; e.g. in the form of building noise and vibration or non-uniform heat transfer, which could tend to reduce the importance of initial conditions.

The subject of initial conditions was first discussed by Foster [5], then by Mahler *et al.*; these authors (especially the latter) concentrated on the set of initial data leading to the fastest growth of the velocity perturbation [as measured by $\bar{w}(t)$]. Such initial conditions simply do not exist; perturbation can be made to grow "as rapidly as desired" by appropriately selecting the initial conditions. Unfortunately, this is somewhat of a negative result in that it weakens the transient theory. It should also be noted that Elder [10] reduced the effect of initial conditions by imposing a continuous random source of temperature perturbations at the surface undergoing the step change.

A "popular" set of initial conditions is that of "white noise", wherein all amplitude coefficients are set equal. In Fig. 3 are shown the temperature and velocity profiles corresponding to white noise for $N = 16$ (thus representing 16 vertical "cells" or "eddies", a rather unlikely configuration). Perhaps the most important feature of white noise is the stronger emphasis given to the perturbations near $z = 0$; since $\partial\bar{T}/\partial z$ is large near $z = 0$, it is reasonable to expect this initial condition to be one of relatively rapid growth. It is also important to note that the initial profiles for white noise vary not only with $N$, the order of the approximation, but also with the type of trial functions employed. The principal reasons given by Foster [5] for selecting white noise were (1) it gave the fastest growth rates, (2) it seemed to be the most reasonable assumption for an arbitrary initial disturbance. Foster, however, overlooked or

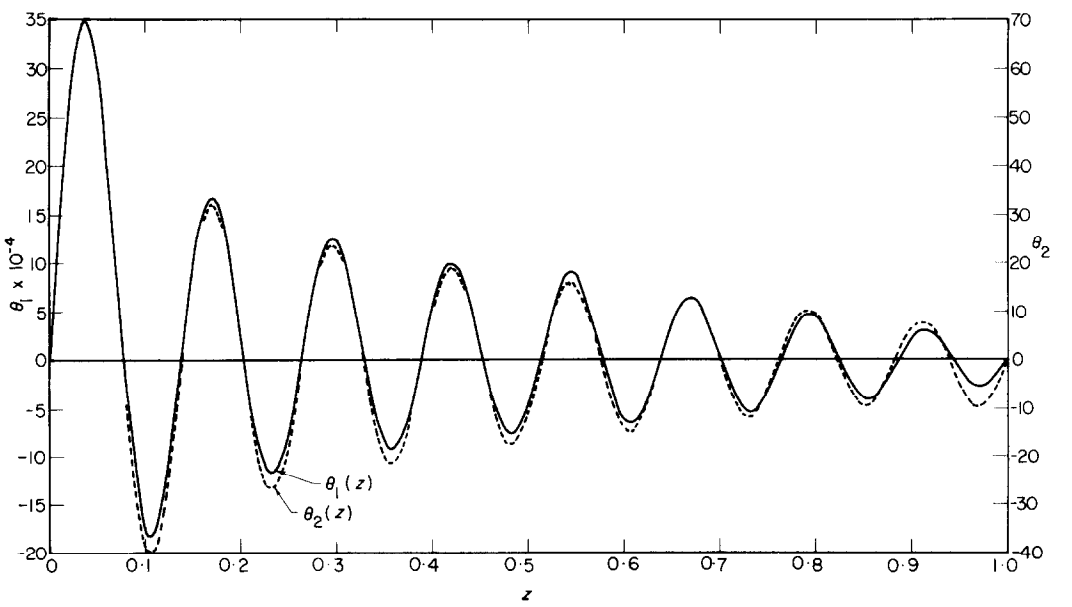


FIG. 4. Initial temperature profiles for two initial conditions for $R = 10^6$, $Pr = 7$, $a = 16$, $N = 16$. Initial conditions: Solid curve—$V_i(0) = 1$, $\dot{V}_i(0) = 10^8$; Dotted curve—$V_i(0) = 1$, $\dot{V}_i(0) = 0$.

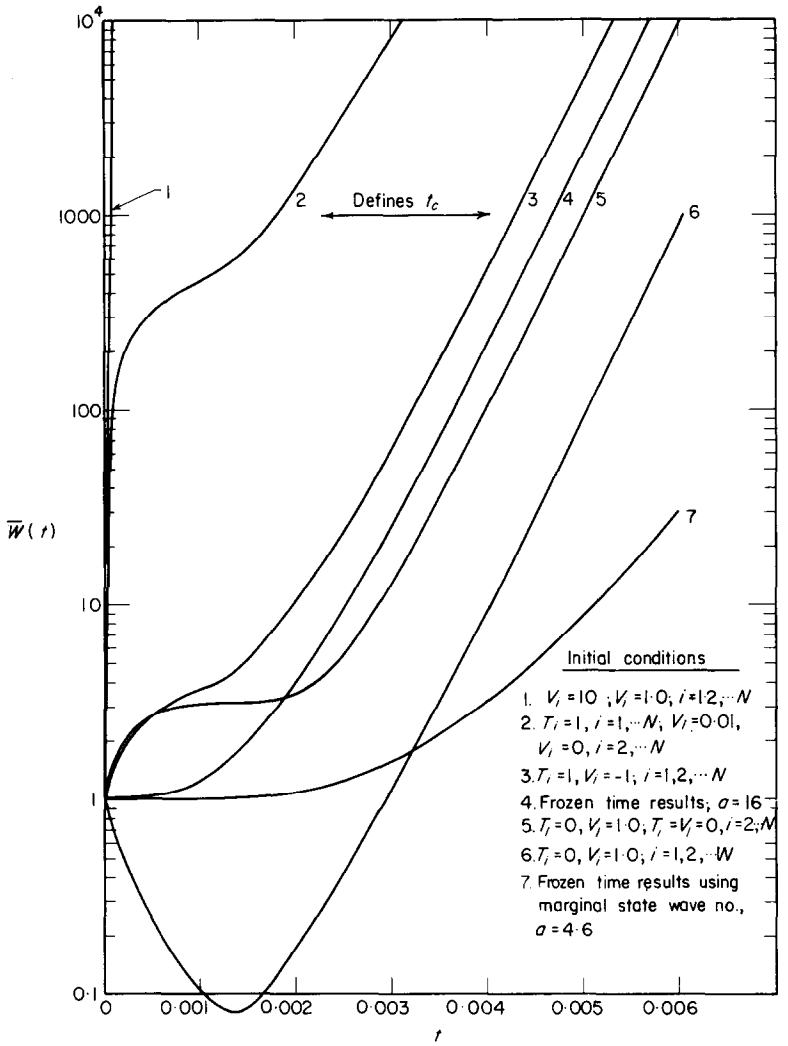


FIG. 5. RMS velocity, $\bar{w}(t)$, for several initial conditions; $R = 10^6$, $Pr = 7$, $a = 16$. $N = 16$.

ignored the fact that his "reasonable" assumption of white noise in velocity with zero slope (acceleration) casued a possibly "unreasonable" distribution of temperature. This effect is a result of combining the two perturbation equations into one higher-order equation and of selecting $\dot{V}_i(0)$ arbitrarily.

In order to obtain a "fastest growing" set of initial data (at least for velocity), the following initial conditions were specified: $\dot{V}_i = 10^8$, $V_i = 1{\cdot}0$, $i = 1, \ldots, N$; this is white noise in velocity with a very large initial slope or acceleration (Foster assumed zero initial slope), the combination admittedly being possible only by specifying an "unusual" temperature distribution. Because of (17) the initial temperature coefficient vector must be

$$\boldsymbol{T} = -\frac{1}{a^2(\sqrt{R})}\mathbf{E}^{-1}.(Pr^{-1}\,\mathbf{C}.\dot{\boldsymbol{V}} + \mathbf{D}.\boldsymbol{V}).$$

The initial acceleration of $10^8$ was selected merely as a dramatic illustration; it should serve

to show, however, that $t_c \to 0$ as $\dot{V}_i(0) \to \infty$, thus precluding the existence of a "fastest-growing" initial condition. In Fig. 4 are shown two initial temperature profiles for white noise in the velocity; the first corresponds to the above example of fast-growing initial conditions and the second to Foster's initial condition of zero slope. It thus turns out that the "forced" temperature profile is really no more "unreasonable" than that corresponding to white noise in temperature (at least for the trial functions employed here).

The results of the investigation of initial conditions are summarized in Fig. 5 for $R = 10^6$, $Pr = 7$, and two "critical" wave numbers—$a = 16$ from the transient results and $a = 4{\cdot}6$ from the frozen time model. (The transient critical wave number is defined to be that which causes $\bar{w}(t)$ to reach 1000 at the earliest time, starting from the same initial data—the frozen time curves will be discussed later.)

Note that the initial conditions can have a significant effect on the onset time, $t_c$; the onset time may vary by as much as $\pm 50$ per cent or more due to initial conditions and moreover, there is no set of fastest growing initial data. However, the importance of the initial condition effect is strongly dependent on the amplification ratio, $\bar{w}(t_c)$, selected to define $t_c$; this is due to the "parallelism" of the curves in Fig. 5. However, the shape of the $\bar{w}(t)$ curves is influenced for a relatively short time only (up to approximately $t = 0{\cdot}0025$ for the data of Fig. 5, $a = 16$); after this time, all curves remain parallel with a slowly increasing slope. It is therefore expected that any reasonable but consistent set of initial data will result in the correct prediction of critical wave number, Prandtl number effect, etc., as long as the transient effects of the initial conditions are minimal by the time the critical value of $\bar{w}(t)$ is reached.

From curves 2 and 6 in Fig. 5, equations (16) and (17), and noting that the transient matrix $\theta(t)$ is zero initially, it is apparent that any initial growth is due to the initial temperature perturbations rather than those on velocity. This is quite reasonable since a temperature perturbation immediately produces buoyancy forces in the fluid, whereas (from the linearized equations) a velocity perturbation can convect energy only after the base temperature gradient becomes appreciable due to thermal diffusion; these processes represent the "driving forces" for the instability, the remaining effects being the diffusive, or stabilizing ones. The onset time may thus be expected to be "small, medium, or large" according to whether the initial disturbance is in the temperature, in both temperature and velocity, or in the velocity only.

Since curves 2 and 6 of Fig. 5 represent fairly reasonable extremes of initial data, and therefore provide "bounds" on the onset time, a single,

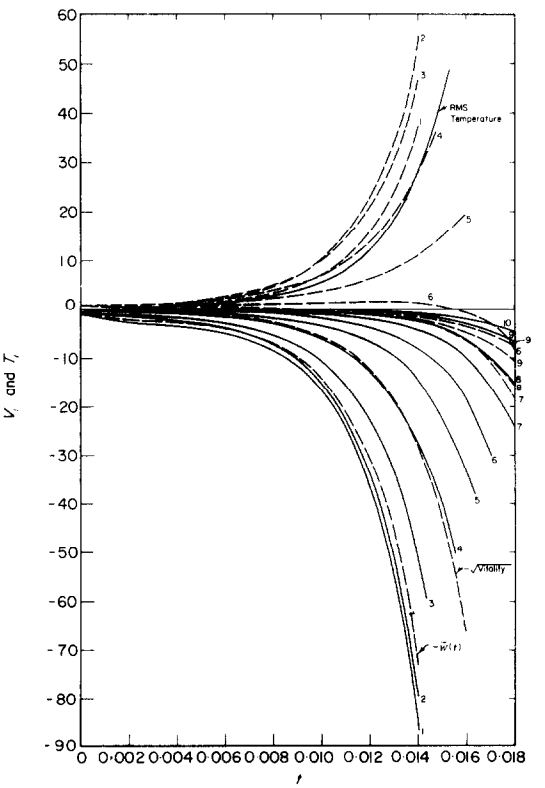


FIG. 6. Growth of the individual amplitude coefficients for $R = 10^5$, $Pr = 7$, $a = 7{\cdot}7$, $N = 10$; $t_c \cong 0{\cdot}02$. White noise initial conditions; $T_i = -V_i = 1{\cdot}0$, $i = 1, 2, \ldots, 10$. The solid, numbered curves are $V_i$ and the dashed, numbered curves at $T_i$.

consistent choice of initial conditions for defining $t_c$ should probably lie between these two extremes. It is not unreasonable, therefore, to select either curve 3 or 5 as the "standard"; the more "active" one of white noise in velocity and temperature (curve 3) was selected.

It must be pointed out, however, that the relative growths of the curves in Fig. 5 apply only to $\bar{w}(t)$; if either the vitality ratio or a root-mean square temperature ratio were used to determine the onset time, the "order" of the curves in Fig. 5 would be changed [e.g. basing the growth on the vitality ratio instead of $\bar{w}(t)$ changes the order from 1, 2, 3, 4, 5, 6 to 4, 2, 3, 5, 1, 6—also, the spread in onset times, $\Delta t_c$, is reduced from approximately 0·006 to approximately 0·0013, thus seemingly giving an "edge" to vitality over $\bar{w}(t)$].

It appears that the dilemma involving initial conditions carries over to the experimental observations of first Blair and Quinn [12] for a step change and second Spangenberg and Rowland [13], Foster [14] and Blair [15] for water evaporation. The difference in the definition of $\bar{w}(t_c)$ in the two types of experiments exceeded four orders of magnitude in order to obtain agreement between experiment and theory.

Figure 6 shows how the amplitude coefficients vary with time compared to the vitality, $\bar{w}(t)$ and RMS temperature for white noise initial data ($T_i = -V_i = 1{\cdot}0$, $i = 1, \ldots, 10$) and $R = 10^5$. A typical feature of the solutions exhibited here is the tendency of the higher-order temperature coefficients to "turn around" as the base temperature profile develops; in the limit of $t \to \infty$ only $T_1$ and $T_2$ will not have reversed their directions.

In contrast to the transient analysis a strongly appealing feature of the frozen time models is that the numerical calculations are quite straightforward and involve no subjective decisions on the part of the analyst. The solution is obtained simply by iteration on $R$ (or $\sigma$) in (18) until the determinant is approximately zero (or changes insignificantly—e.g. to 7–8 decimal places—from one iteration to the next). Thus, for the marginal state analysis ($\sigma = 0$) the minimum $R$ in a plot of $R$ vs. $a$ at a fixed $t$ yields the critical wave number, $a_c$, at the time selected. In the quasi-static analysis it is usually more convenient, though less efficient, to iterate on $\sigma$ at fixed values of $R$, $a$, $t$ and $Pr$; the maximum in a plot of $\sigma$ vs. $a$ (for fixed $R$, $t$, $Pr$) is the (instantaneous) maxima growth rate and is used to define the critical wave number.

## 5. RESULTS AND DISCUSSIONS

Using white noise initial data, several runs were made at various wave numbers for a fixed $R$ and $Pr$—and $\bar{w}(t)$ vs. $t$ was plotted; by cross-plotting the resulting values of time vs. wave number at $\bar{w} = 1000$, both the onset time and critical wave number were obtained from the minimum in the curve. In Figs. 7 and 8 (solid lines) are shown the effect of Rayleigh number on onset time and on the critical wave number, respectively, for $Pr = 7$. It is seen that the infinite layer model could be successfully employed for Rayleigh numbers larger than about $1\text{–}2 \times 10^5$, since the asymptotic conditions have been attained. For these curves, the asymptotic relations are: $Rt_c^{\frac{1}{2}} \cong 280$ and $R \cong 250\, a_c^3$, hence $a_c t_c^{\frac{1}{4}} \cong 1{\cdot}04$ and the scale of the initial motion is thus set by the thickness of the thermal layer (Elder [10]). The numerical coefficients would vary somewhat if different initial conditions were assumed (cf. Fig. 5) or if $\bar{w}(t_c)$ were selected to be other than $10^3$; e.g. for $\bar{w}(t_c) = 10^2$ and $10^4$, the $R$ vs. $t_c$ asymptotes become $Rt_c^{\frac{1}{2}} = 180$ and 380 respectively. These results compare remarkably well with Foster's [8] infinite layer results. From Fig. 1 of his paper, for a slightly different Prandtl number ($Pr = 10$) and different initial conditions, the results are (after converting from the dimensionless units for an infinite depth system to those of this study): $R \cong 230\, a_c^3$ to $250\, a_c^3$ for $\bar{w}(t_c) \cong 10^3$ and $Rt_c^{\frac{1}{2}} \cong 170$, 270 and 360 for $\bar{w}(t_c) = 10^2, 10^3, 10^4$ respectively. This close agreement in onset time

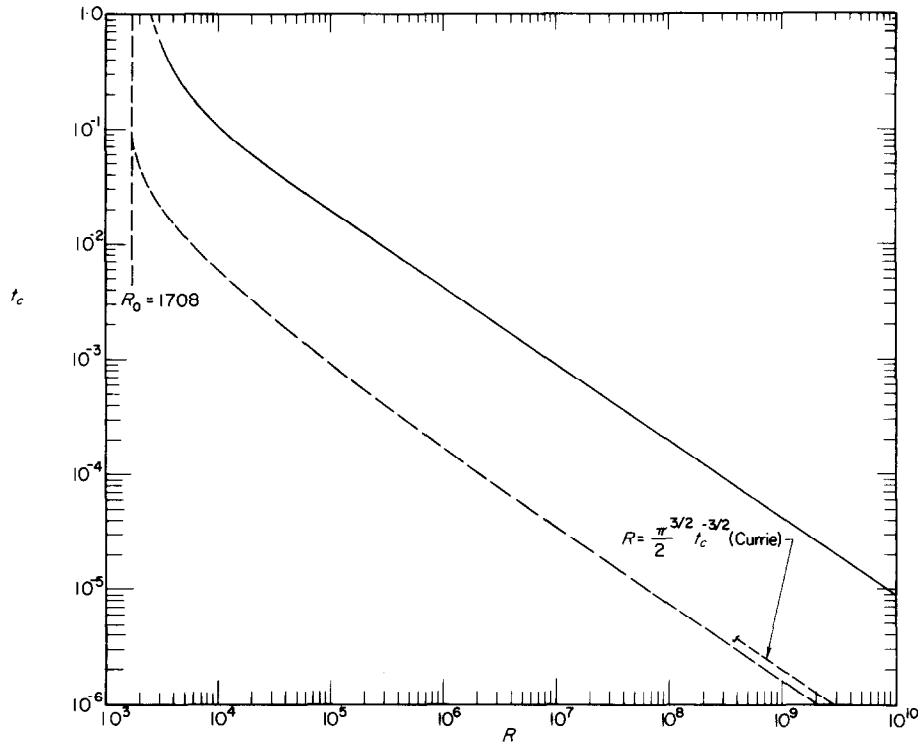


FIG. 7. Onset time vs. Rayleigh number. Solid curves are from transient analysis for $Pr = 7$; dashed curves are from frozen time analysis.

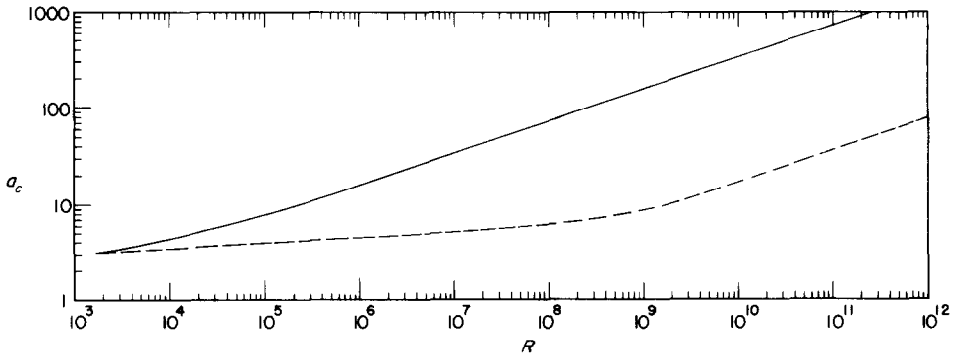


FIG. 8. Critical wave number vs. Rayleigh number. Solid curve is from transient analysis for $Pr = 7$; dashed curves are from frozen time analysis.

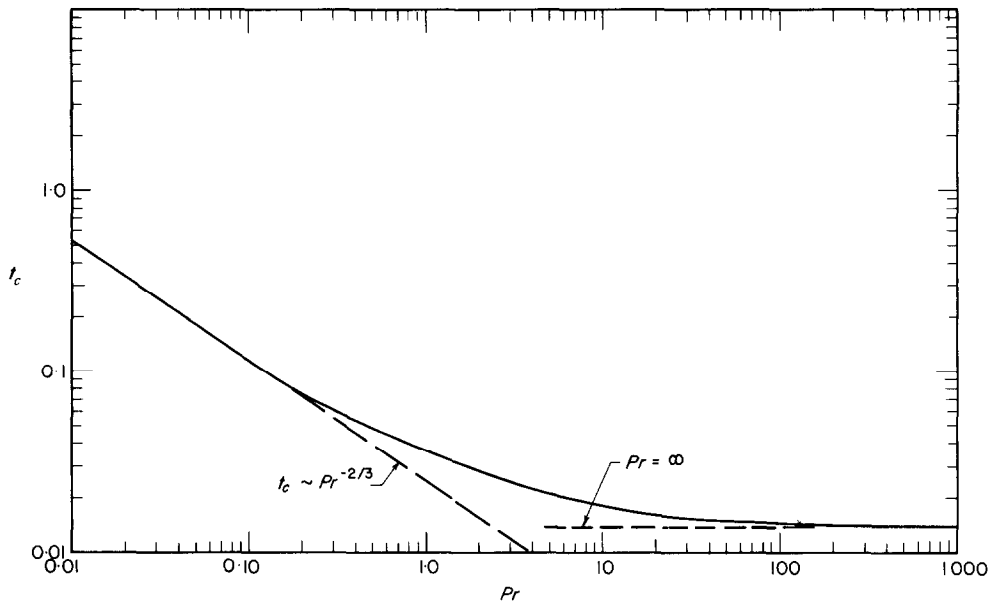


FIG. 9. Variation of onset time with Prandtl number for $R = 10^5$.

is apparently due to the fact that both temperature and velocity perturbations are present initially in each analysis.

The Prandtl number also affects both the onset time and the critical wave number, as shown in Figs. 9 and 10 for $R = 10^5$. For Prandtl numbers greater than about 100, the infinite Prandtl number results seem to apply; i.e. the results are independent of $Pr$ [the values of $t_c \cong 0{\cdot}014$ and $a_c \cong 6{\cdot}75$ from Figs. 9 and 10 may be compared with $t_c \cong 0{\cdot}012$ and $a_c \cong 5{\cdot}8$ from Figs. 3 and 4 of Foster's [8] work for the same $\bar{w}(t_c)$]. For $Pr < \sim 0{\cdot}10$, the onset time varies as $Pr^{-\frac{1}{2}}$ (the asymptote is given by $t_c \,.\, Pr^{\frac{1}{2}} \cong 0{\cdot}0245$); Foster's infinite layer results, for $\bar{w}(t_c) = 10^3$ and $Pr < \sim 0{\cdot}10$ are given approximately by $t_c\,(Pr \,.\, R)^{\frac{1}{3}} = 51$ or $t_c\, Pr^{\frac{1}{3}} \cong 0{\cdot}0237$ for $R = 10^5$. Thus, for small $Pr$ and large $R$, the onset time should vary as $(Pr \,.\, R)^{-\frac{1}{3}}$, which causes the dimensional onset time to be independent of both depth and viscosity (an infinite depth, inviscid fluid). This limiting case would apply as $\nu \to 0$ since this causes $Pr \to 0$ and $R \to \infty$ simultaneously; in this case, as shown by Foster, the dimensional critical wave number is also independent of depth and viscosity, as $a_c \sim (Pr \,.\, R)^{\frac{1}{3}}$. For a finite $R$ however, as in Figs. 9 and 10, these asymptotic results are somewhat different as $Pr \to 0$; while the onset time does vary as $Pr^{-\frac{1}{2}}$, the critical wave number does not vary as $Pr^{\frac{1}{2}}$, but approaches a limit of 3·117. This corresponds to the fastest growing wave number as $Pr \to 0$ for a linear temperature profile and is a result of $t^*c \to \infty$. The interesting "peak wave number", at $Pr = 1$–2 in Fig. 10, was previously predicted by Foster and by Mahler *et al.*

The principal results of the frozen time, marginal state analysis are shown by the dashed lines in Figs. 7 and 8 as onset time and critical wave number as a function of Rayleigh number (for any Prandtl number!). These results were verified via numerical integration of the marginal state ($\sigma = 0$) equations. Here the asymptotic conditions are attained more slowly and are quite different than those from the transient

analysis; for $R > \sim 10^6$, $R\,t_c^{\frac{3}{2}} = 2$ and for $R > \sim 2 \times 10^9$, $R \cong 2{\cdot}04 \times 10^6\ a_c^3$. If these results are interpreted as applying to a fluid layer with a distributed heat source (such that $\partial\overline{T}/\partial t = 0$) which depends on a parameter $t_c$, then they are meaningful. If, however, they are assumed to describe the stability of a fluid layer undergoing a step change in temperature, then, by comparison with the results of the transient analysis, they are clearly seen to be erroneous.

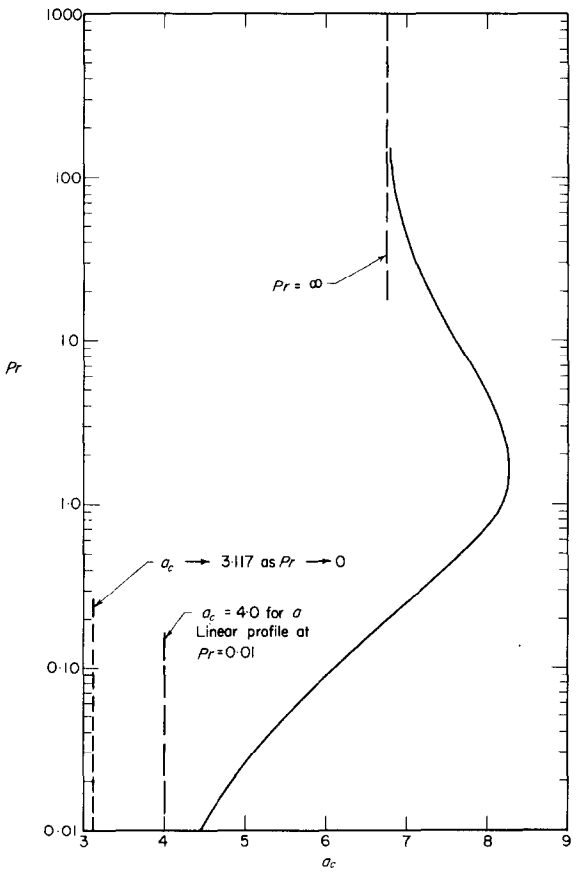


FIG. 10. Critical wave number vs. Prandtl number for $R = 10^5$.

The main reason for the large discrepancy can be traced to the basic premise of the frozen time analysis—it is assumed that the growth rate of the perturbations, $\sigma$, is large compared to the rate of change of the base profile—clearly the worst time to apply this assumption is when $\sigma = 0$; i.e. the basis for the marginal state analysis. For small time, the decay rate, $-\partial\overline{T}/\partial t$, of the base temperature transient varies at most as $1/t$ (at $z = \sqrt{2t}$), while for large time it varies as $e^{-\pi^2 t}$; thus, in general the frozen time model is seen to be relatively poor for small times (large $R$) but gets progressively better for large time (small $R$).

Also shown in Fig. 7 is the asymptote obtained by Currie, $R\,t_c^{\frac{3}{2}} = \pi^{\frac{3}{2}}/2$, which is quite close to the frozen time results of this study. The small difference is most likely attributable to the "thermal depth" approximation employed by Currie. The original approximation suggested by Lick [4], employing two linear segments, should be much closer to being uniformly valid.

Another interesting result obtained by Currie was the prediction of instability for Rayleigh numbers less than 1707·76, depending on the manner and rate of heating. Thus, for a step

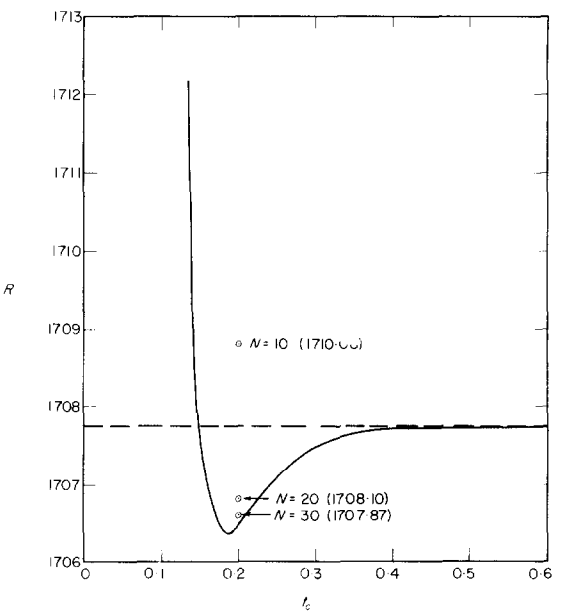


FIG. 11. Frozen time model: Onset time vs. Rayleigh number for large time ($a = 3{\cdot}12$). The solid curve was obtained via numerical integration (50 equal steps in $z$); the other points are from the approximate solution with the corresponding $R$ for a linear profile in parentheses.

change in temperature, his results indicate (potential) instability for $R > 1340$. Although his qualitative prediction of $R < 1707{\cdot}76$ for some range of $t$ is valid, his quantitative predictions, for a step change, are poor. Quantitative values of the critical Rayleigh number are displayed in Fig. 11 and it is apparent that $R$ is less than 1707·76 for $t > \sim 0{\cdot}15$; the minimum of $\sim 1706{\cdot}36$ occurring at $t \cong 0{\cdot}186$. Finally, it should be noted that these results (i.e. $R < 1707{\cdot}76$) are not unusual if they are interpreted as describing the marginal state with a distributed heat source; somewhat similar results were computed by Sparrow *et al.* [17] for a system with a uniform heat source.

Although the frozen time hypothesis is invalid at the marginal state, it may be valid for large time; i.e. when the perturbations are growing rapidly. Hence, the task of selecting a criterion for "sufficiently large time" arises. As a step in this direction, one could compute and plot $\sigma(t)$ for a given Rayleigh number, Prandtl number, and wave number, and "apply" the quasi-static assumption when $(1/\sigma^2)\, d\sigma/dt \leqslant \epsilon$, where $\epsilon$ is "sufficiently small". Such a plot is shown in Fig. 12 for a large Rayleigh number ($10^6$); also plotted are the instantaneous growth rates of the first and tenth individual amplitude coefficients ($T_i$ and $V_i$), where $\sigma(T_i) \equiv \dot{T}_i/T_i$, etc., for the initial conditions $T_1 = -V_1 = 1$; $T_i = V_i = 0$, $i = 2, 3, \ldots, 16$ (the discontinuity in $\sigma(T_{10})$ is caused by $T_{10}$ passing through zero—cf. also Fig. 6). For times on the order of 0·01 or greater, all of the individual growth rates and that from the quasi-static theory tend to converge to about the same value; also

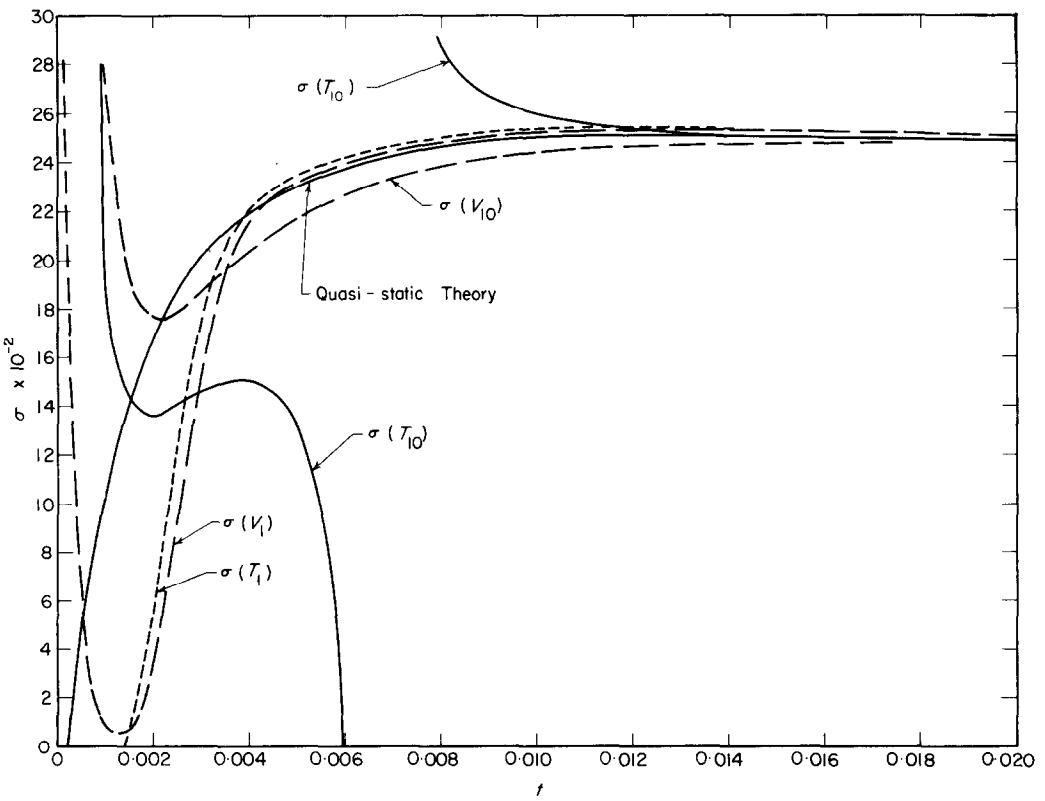


FIG. 12. Growth rates vs. time for $R = 10^6$, $Pr = 7$, $a = 16$, $N = 16$. The marginal state occurs at $t_c = 0{\cdot}00026$ ($\sigma = 0$) from the frozen time model whereas the onset time from the transient model is $t_c = 0{\cdot}0050$ with the initial conditions used here ($T_1 = -V_1 = 1$; others zero).

$(1/\sigma)\,d\sigma/dt$ becomes small compared to 0. Thus, for this particular case, it seems reasonable to conclude that the quasi-static model should be valid for $t > 0{\cdot}01$. However, according to the transient analysis, the onset time for this case is $t_c \cong 0{\cdot}005$ (for white noise initial conditions, $t_c \cong 0{\cdot}0042$ from Fig. 7); i.e. the fluid is already "unstable" by the time the asymptotic theory begins to apply (this is only strictly true for small onset times)—this point was also mentioned first by Foster and later by Elder whose conclusions are more firmly based owing to his inclusion of the nonlinear effects.

## 6. CONCLUSIONS

The results presented here for a finite depth layer undergoining a step change in temperature complement the existing results for a layer of infinite depth with the same boundary conditions (Foster [8]).

The "initial condition effect" may or may not be important depending upon (1) the "type" of initial conditions actually present in a particular laboratory and (2) the amplitude ratio, $\bar{w}(t_c)$, required to correlate the theory with a particular experiment [which varies inversely with both sensitivity of the detection apparatus and the magnitude of $\bar{w}(0)$].

Two "frozen time" models were examined and clarified; it was found that (a) the marginal state analysis is invalid for a fluid layer undergoing a step change in temperature (it does give the neutrally stable solution to "some" problem however; viz. that with the proper distributed heat source), (b) the quasi-static analysis, though valid asymptotically (large time) is of limited usefulness in describing the overall stability of a transient system because in most cases, the linearized equations will cease to become valid by the time that the asymptotic theory becomes valid.

## ACKNOWLEDGEMENTS

This research was supported in part by the National Science Foundation under Grant No. GP-287 which provided funds for the numerical computations and in part by a fellowship received by P. M. Gresho from North American Rockwell Corporation.

## REFERENCES

1. S. CHANDRASEKHAR, *Hydrodynamic and Hydromagnetic Stability*. Clarendon Press, Oxford, (1961).
2. B. R. MORTON, On the equilibrium of a stratified layer of fluid, *J. Mech. Appl. Math.* **10**, 433–447 (1957).
3. A. W. GOLDSTEIN, Stability of a horizontal fluid layer with unsteady heating from below and time-dependent body force, NASA Tech. Report R-4 (1959).
4. W. LICK, The instability of a fluid layer with time-dependent heating, *J. Fluid Mech.* **21**, 565–576 (1965).
5. T. D. FOSTER, Stability of a homogeneous fluid cooled uniformly from above, *Physics Fluids* **8**, 1249–1257 (1965).
6. I. G. CURRIE, The effect of heating rate on the stability of stationary fluids, *J. Fluid Mech.* **20**, 337–347 (1967).
7. J. L. ROBINSON, A note on the stability of an infinite fluid heated from below, *J. Fluid Mech.* **29**, 461–464 (1967).
8. T. D. FOSTER, Effect of boundary conditions on the onset of convection, *Physics Fluids* **11**, 1257–1262 (1968).
9. E. G. MAHLER, R. S. SCHECHTER and E. H. WISSLER, The stability of a fluid layer with time-dependent density gradients, *Physics Fluids* **11**, 1901–1912 (1968).
10. J. W. ELDER, The unstable thermal interface, *J. Fluid Mech.* **32**, 69–96 (1968).
11. S. G. MIKHLIN, *Variational Methods in Mathematical Physics*. Pergamon Press, Oxford (1964).
12. P. M. GRESHO, PhD. Thesis, Universisy of Illinois, Urbana (1969).
13. W. G. SPANGENBERG and W. R. ROWLAND, Convective circulation in water induced by evaporative cooling, *Physics Fluids* **4**, 743–750 (1961).
14. T. D. FOSTER, Onset of convection in a layer of fluid cooled from above, *Physics Fluids* **8**, 1770–1774 (1965).
15. L. M. BLAIR, Ph.D. Thesis, University of Illinois, Urbana (1968).
16. L. M. BLAIR and J. A. QUINN, The onset of cellular convection in a fluid layer with time-dependent density gradients, *J. Fluid Mech.* **36**, 385–400 (1969).
17. E. M. SPARROW, R. J. GOLDSTEIN and V. K. JONSSON, Thermal instability in a horizontal fluid layer: Effect of boundary conditions and non-linear temperature profile, *J. Fluid Mech.* **18**, 513–528 (1964).
18. M. ABRAMORVITZ and I. STEGUN (Editors), *Handbook of Mathematical Functions With Formulas, Graphs and Mathematical Tables*. U.S. Government Printing Office, Washington, D.C. (1964).
19. B. MEISTER, Dte Anfangswertaufgaube für die storungs-differential-gleichungen des Taylorschen Stabilitäts-problems, *Arch. Rat. Mech. Anal.* **14**, 81–107 (1963).

## STABILITÉ D'UNE COUCHE FLUIDE SOUMISE À UN CHANGEMENT ÉCHELON EN TEMPÉRATURE: ANALYSE DU SYSTÈME TRANSITOIRE EN FONCTION DU "TEMPS GELÉ"

**Résumé**—Le comportement linéarisé d'une couche fluide soumise à une variation échelon de température superficielle est examinée à l'aide de deux approches différentes. La première approche utilise des techniques de valeur initiale tandis que la seconde emploie deux versions communes de l'hypothèse de "temps gelé". Les deux surfaces sont choisies rigides et conductrices. La méthode de Galerkin est utilisée afin d'obtenir les solutions approchées tandis que les solutions "exactes" sont obtenues par intégration numérique dans certains cas.

On montre que, tandis que la première version du modèle de "temps gelé" (analyse d'état marginal) n'est pas applicable au système transitoire, la seconde version (analyse quasi-statique) est valable pour une grande durée mais est d'une utilité limitée pour la plupart des cas intéressants. Les effets de conditions initiales variables, sur les perturbations de vitesse et de température, sont clarifiés et discutés. Les résultats présentés ici complètent ceux utilisables pour un fluide semi-infini avec les mêmes conditions aux limites à la surface.

## DIE STABILITÄT EINER FLÜSSIGKEITSSCHICHT, DIE EINEM PLÖTZLICHEN TEMPERATURSPRUNG UNTERWORFEN WIRD: INSTATIONÄRE UND QUASISTATIONÄRE BEHANDLUNG

**Zusammenfassung**—Das linearisierte Verhalten einer Flüssigkeitsschicht, deren Oberflächentemperatur eine sprunghafte Änderung erfährt, wird mit zwei verschieden konzipierten Näherungsverfahren untersucht. Das erste Verfahren arbeitet mit der Anfangswerttechnik, während das zweite zwei übliche Methoden der "frozen-time"-Hypothese anwendet. Beide Oberflächen werden als starr und leitend angenommen. Galerkins Methode wird verwendet, um Näherungslösungen zu erhalten, während "exakte" Lösungen in bestimmten Fällen mit numerischer Integration erreicht werden.

Es zeigt sich, dass die erste Version des "frozen-time"-Modells (Randwertanalyse) auf das Übergangssystem nicht anwendbar ist, während die zweite Version (quasistatische Analyse) für eine lange Zeit gültig ist, aber für die meisten interessierenden Fälle begrenzten Nutzen hat. Die Einflüsse verschiedener Anfangsbedingungen auf Geschwindigkeits- und Temperaturstörungen werden geklärt und diskutiert. Die hier erzielten Ergebnisse vervollständigen jene, die für eine halbunendliche Flüssigkeitsschicht mit denselben Randbedingungen an der Oberfläche angegeben sind.

## УСТОЙЧИВОСТЬ ЖИДКОГО СЛОЯ ПРИ СТУПЕНЧАТОМ ИЗМЕНЕНИИ ТЕМПЕРАТУРЫ

**Аннотация**—Линеаризованное поведение жидкого слоя при ступенчатом изменении температуры поверхности рассматривается с использованием двух различных подходов. При первом подходе исходят из краевой задачи с начальными условиями, тогда как при втором используются два обычных варианта гипотезы «замороженного времени». Обе поверхности принимаются жесткими и проводящими. Для получения приближенных решений используется метод Галеркина, а «точные» решения получены путем численного интегрирования для определенных случаев.

Показано, что если первый вариант модели замороженного времени / анализ краевых состояний / не применим для переходных процессов в системе, то второй вариант / квазистатический анализ / справедлив для больших времен, но он ограниченно полезен для большинства интересных случаев. Найдено и обсуждается влияние различных начальных условий на возмущения скорости и температуры. Результаты, представленные в данной статье, дополняют имеющиеся данные для полубесконечной жидкости с теми же граничными условиями у верхней поверхности.